Phytochemistry 177 (2020) 112449

Contents lists available at ScienceDirect

Phytochemistry

journal homepage: www.elsevier.com/locate/phytochem

Mexicanolide-type limonoids from the twigs and leaves of *Cipadessa baccifera*

Dong-Hua Cao[a,b,f], Shang-Gao Liao[c], Peng Sun[a,b], Yi-Dian Xiao[d,e], Chun-Fen Xiao[a], Hua-Bin Hu[a], Wolfram Weckwerth[f,g], You-Kai Xu[a,*]

[a] Key Laboratory of Tropical Plant Resources and Sustainable Use, Xishuangbanna Tropical Botanical Garden, Chinese Academy of Sciences, Menglun, 666303, PR China
[b] University of Chinese Academy of Sciences, Beijing, 100049, PR China
[c] State Key Laboratory of Functions and Applications of Medicinal Plants & School of Pharmacy, Guizhou Medical University, Guizhou, 550025, PR China
[d] State Key Laboratory of Phytochemistry and Plant Resources in West China, Kunming Institute of Botany, Chinese Academy of Sciences, Kunming, 650201, PR China
[e] School of Chemical Science and Technology, Key Laboratory of Medicinal Chemistry for Nature Resource, Ministry of Education, Yunnan University, Kunming, 650091, PR China
[f] Department of Ecogenomics and Systems Biology, University of Vienna, Althanstrasse 14, Vienna, 1090, Austria
[g] Vienna Metabolomics Center (VIME), University of Vienna, Althanstrasse 14, Vienna, 1090, Austria

ARTICLE INFO

Keywords:
Cipadessa baccifera
Meliaceae
Mexicanolide-type limonoid
Structure elucidation
Biological activity

ABSTRACT

Twelve previously undescribed mexicanolide-type limonoids, including two pairs of isomers, together with seven known analogues were isolated from the twigs and leaves of *Cipadessa baccifera*. Their structures were determined by extensive spectroscopic methods and electronic circular dichroism (ECD) calculations. Structural variations mainly occurred at the attachment of C-3 and the carbon residues linked to C-17. 21-deoxo-23-oxofebrifugin A and 3-*O*-detigloyl-3-*O*-isobutyryl-21-deoxo-23-oxofebrifugin A are two rare naturally occurring mexicanolide-type limonoids bearing an *α,β*-unsaturated-γ-lactone motif at C-17. Moreover, cipaferen R is the first degraded tetranortriterpenoid derivative featuring an unique acetyl group at C-17. Some isolated compounds were evaluated for nematicidal, antifungal, cytotoxic (against five human cancer cell lines), and acetylcholinesterase inhibitory activities. No nematicidal and antifungal activities were observed, yet 3-*O*-detigloyl-3-*O*-isobutyrylfebrifugin A, febrifugin A, febrifugin, and khaysin T exhibited moderate cytotoxic activity against the tested cells with IC_{50} values ranging from 18.56 ± 0.27 to 38.00 ± 0.85 μM, and 3-*O*-detigloyl-3-*O*-isobutyrylfebrifugin A, granatumin E, khaysin T, and 2′*S*-cipadesin A showed moderate inhibitory activities against acetylcholinesterase (AChE) at 50 μM.

1. Introduction

The genus *Cipadessa* (family: Meliaceae) includes four documented species, *C. baccifera* (Roth) Miq., *C. cinerascens* (Pellegr.) Hand-Mazz., *C. fruticosa* Blume, and *C. boiviniana* Baill.. Previously, it was sorted in the tribe Turraeeae by Harms but was finally placed in the tribe Trichileae of the Melioideae subfamily based on its vegetative, floral, fruit, and pollen characteristics (Pennington and Styles, 1975). *C. baccifera* (Roth) Miq. is a bushy shrub with pinnate leaves mainly distributed in tropical Asia, such as India, Indonesia, Malaysia, Thailand, and southern China (Chen et al., 1997). In India, although the wood of the plant is used as fuel, its leaves and fruits are used as cattle fodder or fish poison, and the whole plant is used to treat diabetes, diarrhoea, headaches, piles, snake poison, and psoriasis (Malarvannan et al., 2009). A paste with its leaves and stem bark, along with goat's milk, as the major ingredient is administered orally for wounds (Ram et al., 2004). "Ya Luo Qing", which is prepared from the leaves and roots of *C. baccifera* and *C. cinerascens*, has been traditionally used as folk medicine by Dai people in Xishuangbanna, Southwest, China for treatment of various diseases such as dysentery, malaria, pruritus (itchy skin), rheum, rheumatism, and burns and scalds (Jiangsu New Medical College, 1977). Previous phytochemical researches on *Cipadessa* species have led to the isolation of structurally diverse limonoids (e.g., mexicanolides, methyl angolensates, trijugins, and cipadesins), some of which exhibited a wide range of biological effects including antimalarial, antioxidant, antimicrobial, cytotoxic, insecticidal, and trypanocidal activities (Bandi and Lee, 2012; Siva et al., 2014, 2017; Yu et al., 2015, 2018).

Limonoids, a class of highly oxygenated and modified nortriterpenoids widely found in the plants of Meliaceae and Rutaceae

* Corresponding author.
E-mail address: xyk@xtbg.ac.cn (Y.-K. Xu).

https://doi.org/10.1016/j.phytochem.2020.112449
Received 16 October 2019; Received in revised form 28 May 2020; Accepted 11 June 2020
Available online 26 June 2020
0031-9422/

families, have attracted considerable attention from both the medicinal chemists and chemical biologists due largely to their fascinating structural diversity and extensive biological activities (Liao et al., 2009; Tan and Luo, 2011). In the continuing search for biologically active limonoids from Meliaceae plants, twelve previously undescribed limonoids and seven known analogues were isolated from the leaves and twigs of *C. baccifera*. Their structures with the absolute configurations were established by extensive spectroscopic analyses and ECD calculations. Some isolated compounds were evaluated for their nematicidal, antifungal, cytotoxic (against five human cancer cell lines), and acetylcholinesterase inhibitory activities.

2. Results and discussion

The 95% ethanol extract of *C. baccifera* was subjected to silica gel column chromatography (CC), Sephadex LH-20 CC, and semi-preparative HPLC to yield nineteen compounds including twelve previously undescribed limonoids (**1–12**) and seven known analogues (**13–19**). The known compounds were identified to be febrifugin A (**13**) (Leite et al., 2005), granatumin E (**14**) (Li et al., 2009), cipaferen M (**15**) (Siva et al., 2014), febrifugin (**16**) (Rao et al., 1978), khaysin T (**17**) (Siva et al., 2014), 2′*S*-cipadesin A (**18**) (Gan et al., 2007), and ruageanin A (**19**) (Mootoo et al., 1996), respectively, by comparing their spectroscopic data with those reported in the literature.

Compound **1** was obtained as a white amorphous powder. Its molecular formula $C_{31}H_{40}O_{10}$ was established on the basis of the negative HRESIMS peak at *m/z* 571.2548 $[M - H]^-$ (calcd. for $C_{31}H_{39}O_{10}$, 571.2549), indicating the presence of 12 degrees of unsaturation. The IR absorptions at 3433, 1770, 1727, and 1634 cm^{-1} showed the presence of hydroxyl, γ-lactone, carbonyl, and olefinic groups, respectively. The ^{13}C NMR data (Table 3) displayed 31 carbon resonances, which were further classified by the DEPT experiment as seven methyls (one *O*-methyl), four methylenes, ten methines (two olefinic and three oxygenated), and ten quaternary carbons (two olefinic and five carbonyls). A 23-hydroxybutenolide moiety (δ_H 7.33, br s; 6.18 br s; δ_C 168.4, 149.5, 135.5, and 92.0), an isobutyryloxy group (δ_H 2.63, m; 1.17, d, J = 7.2 Hz; 1.17, d, J = 7.2 Hz; δ_C 176.8, 34.0, 19.4, and 18.7), a trisubstituted double bond (δ_H 5.35, d, J = 6.7 Hz; δ_C 138.0 and 123.3), one ketocarbonyl (δ_C 217.3), and four ester carbonyls (δ_C 176.8, 173.9, 168.6, and 168.4) were evident from the NMR data (Tables 1 and 3). Those identified functionalities accounted for 8 out of 12 degrees of unsaturation, thus requiring four additional rings in the structure of **1**. These observations suggested that **1** possessed the same mexicanolide-type carbon skeleton as febrifugin A (Leite et al., 2005), with the only difference being the presence of an isobutyryloxy group instead of a tigloyloxy group at C-3. This deduction was further validated by 2D NMR data (Fig. 2). The carbon resonance at δ_C 217.3 was assigned to C-1 by the HMBC correlations from H-2/Me-19/H-30 to C-1. The multiple HMBC correlations from H-3/Me-3′/Me-4′ to C-1′ indicated that the isobutyryloxy group was attached to C-3. The HMBC correlations from the methoxyl (δ_H 3.66) to C-7 (δ_C 173.9) and from H_2-6 to C-5/C-7 placed the methoxycarbonyl group at C-6. The $\Delta^{8(30)}$ double bond was fixed by the HMBC correlations from H-30 to C-1/C-3/C-9/C-14. The 23-hydroxybutenolide moiety was attached to C-17 based on the HMBC correlations from H-17 (δ_H 5.60) to C-20 (δ_C 135.5)/C-21 (δ_C 168.4)/C-22 (δ_C 149.5). The planar structure of **1** was thus confirmed.

The relative configuration of **1** was established by ROESY correlations (Fig. 2B) and by comparing the NMR data with those of febrifugin A (Leite et al., 2005). Suppose H-2 was α-oriented as in all mexicanolide-type limonoids, the coupling constant of 9.3 Hz comparable to those of febrifugin A between H-2 and H-3 suggested an α-orientation for H-3. The ROESY correlations of H-2/H-3, H-3/Me-28, H-9/Me-19, H-9/H-11*α*, H-14/Me-18, and Me-18/H-15*α* indicated that these protons were all *α*-oriented. While the ROESY correlations of H-5/H-17, H-5/H-11*β*, H-17/H-11*β*, and H-5/Me-29 revealed a *β*-orientation for the corresponding protons/groups. The relative stereochemistry of C-23 could not be assigned *via* the available NMR data. Thus, the structure of **1** was established and was named 3-*O*-detigloyl-3-*O*-isobutyrylfebrifugin A.

Compound **2**, a white amorphous powder, possessed a molecular formula of $C_{32}H_{42}O_{10}$ as deduced from the positive HRESIMS peak at *m/z* 609.2674 $[M + Na]^+$ (calcd. for $C_{32}H_{42}O_{10}Na$, 609.2670), showing 14 mass units more than that of **1**. The IR absorptions at 1774, 1728, and 1623 cm^{-1} indicated the presence of γ-lactone, carbonyl, and olefinic groups, respectively. A comparison of the 1D NMR data (Table 1 and 3) of **2** with those of **1** indicated they shared similar structural skeleton. However, an additional methyl singlet (δ_H 3.59, s) and distinct chemical shifts of the proton (δ_H from 6.18 to 5.79 for H-23) and carbon (δ_C from 92.0 to 102.5 for C-23) were observed, suggesting the presence of a 23-methoxybutenolide moiety at C-17 in **2**. This conclusion was confirmed by the MS data together with the HMBC correlations from H-17 (δ_H 5.59, s) to C-20 (δ_C 136.1)/C-21 (δ_C 168.3)/C-22 (δ_C 147.9) and from $OC\underline{H}_3$-23 (δ_H 3.59, s) to C-23 (δ_C 102.5). The relative configuration of **2** were assigned the same as those of **1** on the basis of ^1H NMR data and ROESY spectrum (Supporting Information Fig. S19). The structure of **2** was thereby elucidated and was named 3-*O*-detigloyl-3-*O*-isobutyryl-23-*O*-methylfebrifugin A.

Compound **3** was an isomer of **1** with the same molecular formula of $C_{31}H_{40}O_{10}$, as determined by the negative HRESIMS peak at *m/z* 571.2546 $[M - H]^-$ (calcd. for, $C_{31}H_{39}O_{10}$, 571.2549). Analysis of the 1D NMR data (Tables 1 and 3) revealed that both compounds shared similar structures with the major change in ring E. Signals for a 23-hydroxybutenolide moiety (δ_H 7.33, s; 6.18, s; δ_C 168.4, 149.5, 135.5, and 92.0) in **1** were replaced by those for a 21-hydroxybutenolide one (δ_H 6.29, s; 6.10, s; δ_C 169.2, 163.1, 122.2, and 97.5) at C-17 in **3**. The relative configuration in the limonoid core of **3** was assigned to be same as those of **1** based on its ROESY data (Supporting Information Fig. S29). The relative configuration of C-21 could not be assigned *via* the available NMR data. Granatumin E (**14**) was an isomer of febrifugin A (**13**). Thus, the structure of **3** was assigned and named 3-*O*-detigloyl-3-*O*-isobutyrylgranatumin E.

Compound **4** was an isomer of **2** with the same molecular formula of $C_{32}H_{42}O_{10}$ as deduced from the positive HRESIMS peak at *m/z* 609.2668 $[M + Na]^+$ (calcd. for $C_{32}H_{42}O_{10}Na$, 609.2670). The NMR data (Tables 1 and 3) indicated that **4** had a structure similar to **2**. The only difference involved the substituent at C-17, where **4** bore a 21-methoxybutenolide moiety (δ_H 6.36, s; 6.09, s; δ_C 169.5, 162.0, 125.4, and 104.0) instead of a 23-methoxybutenolide moiety (δ_H 7.22, br s; 5.79, br s; δ_C 168.3, 147.9, 136.1, and 102.5) in **2**. This conclusion was further verified by the HMBC and ROESY data (Supporting Information Fig. S39). The structure of **4** was thus established and was named 3-*O*-detigloyl-3-*O*-isobutyryl-21-*O*-methylgranatumin E.

Compound **5**, obtained as a white amorphous powder, possessed a molecular formula of $C_{30}H_{38}O_{10}$ as assigned by the positive HRESIMS peak at *m/z* 581.2359 $[M + Na]^+$ (calcd. for $C_{30}H_{38}O_{10}Na$, 581.2357). Its ^1H and ^{13}C NMR data (Tables 1 and 3) were similar to those of granatumin E (Wang et al., 2013), except for the presence of signals for a propanoyl group (δ_H 2.42, m; 2.39, m; 1.14, overlapped; δ_C 174.2, 27.1, and 9.0) instead of those for the tigloyloxy group at C-3, which was confirmed by the HMBC correlation of H-3/C-1′. The structure of **5** was thus established and was named 3-*O*-detigloyl-3-*O*-propanoylgranatumin E.

Compound **6** was obtained as a white amorphous powder with a molecular formula of $C_{33}H_{42}O_{10}$ on the basis of the negative HRESIMS peak at *m/z* 597.2707 $[M - H]^-$ (calcd. for $C_{33}H_{41}O_{10}$, 597.2705). The 1D NMR data of **6** (Tables 1 and 3) closely resembled those of **4**. Whereas, signals for the isobutyryloxy group in **4** were replaced by those for a tigloyloxy group (δ_H 6.88, q; 1.85, d; 1.84, s; δ_C 167.1, 139.3, 127.8, 14.9, and 12.0) in **6**, suggesting a 3-tigloyloxy derivative of **4**. The above assignments were further confirmed by 2D NMR data, especially HMBC correlations (Supporting Information Fig. S59), where the key correlations from H-3/H-3' (δ_H 6.88)/Me-4′ to C-1′ were

Table 1
^{1}H NMR spectroscopic data for compounds **1–6.**

NO.	1[a]	2[b]	3[a]	4[b]	5[b]	6[b]
	(mult., *J* in Hz)	(mult., *J* in Hz)	(mult., *J* in Hz)	(mult., *J* in Hz)	(mult., *J* in Hz)	(mult., *J* in Hz)
2	3.47, overlapped	3.49, overlapped	3.53, overlapped	3.49, overlapped	3.52, overlapped	3.49, dd (9.4, 7.0)
3	4.74, d (9.3)	4.74, d (9.4)	4.77, d (9.5)	4.75, d (9.3)	4.78, d (9.5)	4.82, d (9.4)
5	3.43, d (10.3)	3.45, d (10.4)	3.26, d (10.4)	3.32, d (9.8)	3.20, d (8.8)	3.37, d (9.8)
6*α*	2.35, dd (17.2, 10.3)	2.34, dd (17.3, 10.4)	2.42, dd (17.1, 10.4)	2.37, dd (16.7, 9.8)	2.43, m	2.36, dd (17.1, 9.8)
6*β*	2.44, d (17.2)	2.45, d (17.3)	2.35, d (17.1)	2.33, d (16.7)	2.37, m	2.31, d (17.1)
9	2.23, overlapped	2.28, dd (13.4, 3.8)	2.25, overlapped	2.25, dd (12.2, 4.3)	2.25, overlapped	2.23, dd (13.2, 5.0)
11*α*	1.75, m	1.74, m	1.80, m	1.68, m	1.76, m	1.74, m
11*β*	2.23, overlapped	2.30, m	2.06, m	1.97, m	2.07, m	2.08, dd (13.2, 3.7)
12*α*	1.91, d (14.2)	1.92, dt (14.5, 4.4)	1.65, m	1.42, td (14.4, 4.2)	1.65, td (14.3, 4.4)	1.59, m
12*β*	1.44, m	1.44, td (14.5, 4.4)	1.80, m	2.19, d (14.4)	2.13, m	1.84, m
14	2.23, overlapped	2.22, overlapped	2.25, overlapped	2.24, overlapped	2.25, overlapped	2.20, overlapped
15*α*	2.85, dd (18.1, 7.2)	2.85, overlapped	2.86, overlapped	2.86, dd (18.5, 5.9)	2.88, overlapped	2.82, dd (18.8, 6.0)
15*β*	2.84, d (18.1)	2.83, overlapped	2.81, overlapped	2.79, d (18.5)	2.78, overlapped	2.76, d (18.8)
17	5.60, s	5.59, s	5.56, s	5.57, s	5.57, s	5.63, s
18	1.04, s	1.02, s	1.13, s	1.12, s	1.14, s	1.07, s
19	1.14, s	1.16, s	1.15, s	1.15, s	1.13, s	1.16, s
21			6.10, s	6.09, s	6.10, s	5.90, s
22	7.33, br s	7.22, br s	6.29, s	6.36, s	6.30, s	6.18, s
23	6.18, br s	5.79, br s				
28	0.80, s	0.80, s	0.83, s	0.81, s	0.82, s	0.82, s
29	0.77, s	0.78, s	0.77, s	0,76, s	0.76, s	0.78, s
30	5.35, d (6.7)	5.35, d (6.8)	5.36, d (7.0)	5.35, d (6.8)	5.35, d (7.1)	5.32, d (7.0)
OMe-7	3.66, s	3.64, s	3.73, s	3.71, s	3.72, s	3.67, s
OMe-21				3.50, s		3.62, s
OMe-23		3.59, s				
2′	2.63, m	2.61, m	2.62, m	2.63, m	2.39, m 2.42, m	
3′	1.17, d (7.2)	1.17, d (7.1)	1.17, d (5.8)	1.17, d (7.1)	1.14, overlapped	6.88, q (7.5)
4′	1.17, d (7.2)	1.18, d (7.0)	1.17, d (5.8)	1.17, d (6.8)		1.84, s
5′						1.85, d (6.2)

[a] Recorded in $CDCl_3$ at 500 MHz for ^{1}H NMR.
[b] Recorded in $CDCl_3$ at 600 MHz for ^{1}H NMR.

observed. Thus, the structure of **6** was established and was named 21-*O*-methylgranatumin E.

Compounds **7** and **8** had the molecular formulas of $C_{31}H_{40}O_{11}$ and $C_{32}H_{42}O_{11}$, respectively, on the basis of their negative HRESIMS peak at *m/z* 587.2498 [M − H]$^-$ (calcd. for $C_{31}H_{39}O_{11}$, 587.2498) and 601.2654 [M − H]$^-$ (calcd. for $C_{32}H_{41}O_{11}$, 601.2654). The ^{1}H and ^{13}C NMR data (Tables 2 and 3) of **7** and **8** were close to those of ruageanin A (**19**), a mexicanolide-type limonoid with a $\Delta^{8,30}$ epoxide ring isolated from *Ruagea glabra* (Mootoo et al., 1996). The common difference were the presence of signals for a 23-hydroxybutenolide moiety and absence of signals for a *β*-furan ring at C-17 in **7** and **8**. Besides, signals for the isobutyryloxy group (δ_H 2.75, m; 1.28, d, J = 7.0 Hz; 1.26, d, J = 7.0 Hz; δ_C 176.0, 34.2, 19.5, and 18.9) at C-3 in ruageanin A (**19**) were replaced by those for a 2′*R*-methylbutanoate group (δ_H 2.55, m; 1.76, m; 1.51, m; 1.25, d, J = 7.0 Hz; 0.97, t, J = 7.0 Hz; δ_C 175.7, 41.7, 26.8, 17.5, and 12.1) in **8**. These above assignments were further confirmed by the HMBC data (Supporting Information Figs. S69 and S79). According to the general ruler (Gan et al., 2007), comparison of the spectroscopic data of **8** with those reported for cipadessain F revealed that **8**, with a 2′*R*-configuraton, was identical to cipadessain F (Sun et al., 2018), as determined by their very similar chemical shifts of Me-4′ and Me-5′ and the ROSEY correlation of H-2'/H-15*α* (Supporting Information Fig. S79). The relative configurations in the limonoid core of **7** and **8** were assigned to be same as those of ruageanin A based on its ^{1}H NMR data and ROESY data (Supporting Information Figs. S69 and S79). The relative configuration of C-23 could not be assigned via the available NMR data. The structures of **7** and **8** were thus established and were named 21-oxo-23-hydroxylruageanin A and 3-*O*-detigloyl-3-*O*-(2′*R*-methylbutanoyl)-21-oxo-23-hydroxylruageanin A, respectively.

Compound **9**, a white amorphous solid, gave a molecular formula of $C_{32}H_{38}O_{11}$ as deduced from the negative HRESIMS peak at *m/z* 597.2345 [M − H]$^-$ (calcd. for $C_{32}H_{37}O_{11}$, 597.2341), indicating the presence of 14 degrees of unsaturation. Its ^{1}H and ^{13}C NMR data (Tables 2 and 3) were very close to those of **8**. Whereas, except for the presence of an $\Delta^{14(15)}$ double bond in **9**, signals for the 2′*R*-methylbutanoate group (δ_H 2.55, m; 1.76, m; 1.51, m; 1.25, d, J = 7.0 Hz; 0.97, t, J = 7.0 Hz; δ_C 175.7, 41.7, 26.8, 17.5, and 12.1) in **8** were replaced by those for a tigloyloxy group (δ_H 7.05, q; 1.95, s; 1.93, d, J = 7.1 Hz; δ_C 166.7, 140.1, 128.0, 15.0, and 12.5) in **9**, suggesting that **9** differs from **8** in the C-3 substituent and $\Delta^{14(15)}$ double bond. Thus, **9** was likely a 3-tigloyloxy derivative of **8**. This was confirmed by the 2D NMR spectra (including HMBC and ROESY, Supporting Information Fig. S89). The tigloyloxy group was attached at C-3, which was confirmed by the HMBC correlations from H-3/H-3'/Me-4′ to C-1'. The $\Delta^{14(15)}$ double bond was verified by the HMBC correlations from H-15 (δ_H 6.11) to C-8/C-13/C-14/C-16. Thus, the structure of **9** was established and was named 3-*O*-deisobutyryl-3-*O*-tigloyl-14,15-dedihydro-21-oxo-23-hydroxylruageanin A.

Compound **10** was obtained as a white amorphous powder, having a molecular formula of $C_{32}H_{40}O_9$ as determined by the negative HRESIMS peak at *m/z* 567.2600 [M − H]$^-$ (calcd. for $C_{32}H_{39}O_9$, 567.2600). Comparison of its 1D NMR data (Tables 2 and 3) with those of febrifugin (**16**) (Rao et al., 1978), indicated that they had the very similar rings A, B, C, and D with the only difference occurring in the ring E, where an *α,β*-unsaturated-γ-lactone ring (δ_H 6.21, s, 1H; 4.98, m, 2H; δ_C 172.2, 163.8, 118.6, and 72.1) in **10** replaced the 23-hydroxybutenolide moiety (δ_H 7.34, s; 6.21, s; δ_C 168.4, 149.5, 135.4, and 97.0) in febrifugin A. This conclusion was verified by the HMBC correlations from H-17 (δ_H 5.73) to C-20 (δ_C 163.8)/C-21 (δ_C 72.1)/C-22 (δ_C 118.6) and from H_2-21 (δ_H 4.98) to C-20 (δ_C 163.8)/C-22 (δ_C 118.6)/C-23 (δ_C 172.2) (Supporting Information Fig. S99). The relative configuration of **10** was established as the same as that of febrifugin from the very similar ^{1}H NMR coupling patterns and ROESY data (Supporting Information Fig. S99). The structure of compound **10** was

Table 2
^{1}H NMR spectroscopic data for compounds **7–12.**

NO.	7[a]	8[b]	9[b]	10[b]	11[a]	12[b]
	(mult., *J* in Hz)	(mult., *J* in Hz)	(mult., *J* in Hz)	(mult., *J* in Hz)	(mult., *J* in Hz)	(mult., *J* in Hz)
2	3.56, dd (9.4, 2.3)	3.56, dd (9.4, 2.1)	3.66, dd (9.2, 2.0)	3.53, dd (9.3, 6.8)	3.51, overlapped	3.49, overlapped
3	5.09, d (9.4)	5.08, d (9.4)	5.10, d (9.2)	4.82, d (9.3)	4.77, d (9.4)	4.81, d (9.3)
5	3.22, dd (7.5, 5.8)	3.20, dd (6.6, 5.0)	3.42, d (9.6)	3.37, d (9.5)	3.32, d (9.6)	3.37, d (10.6)
6*α*	2.36, dd (16.4, 5.8)	2.36, dd (16.6, 5.0)	2.33, dd (18.6, 9.6)	2.38, dd (17.3, 9.5)	2.38, dd (16.5, 9.6)	2.35, dd (17.0, 10.6)
6*β*	2.35, dd (16.4, 7.5)	2.35, dd (16.6, 6.6)	2.30, d (18.6)	2.33, d (17.3)	2.36, d (16.5)	2.38, d (17.0)
9	1.91, dd (13.0, 5.8)	1.89, dd (13.2, 5.4)	1.96, overlapped	2.26, overlapped	2.27, overlapped	2.21, dd (10.6, 5.0)
11*α*	1.82, m	1.82, m	1.76, m	1.74, m	1.76, m	1.72, m
11*β*	1.83, m	1.83, m	1.50, m	2.04, m	2.06, m	2.08, m
12*α*	2.20, dt (14.9, 2.8)	2.23, dt (15.2, 3.2)	1.25, m	1.60, m	1.63, m	1.41, td (17.4, 4.0)
12*β*	1.16, m	1.15, m	2.21, m	1.83, m	1.84, m	2.26, m
14	1.52, dd (15.2, 4.5)	1.50, dd (15.1, 4.3)		2.24, overlapped	2.27, overlapped	2.10, overlapped
15*α*	2.83, dd (15.9, 4.5)	2.83, dd (15.8, 4.3)	6.11, s	2.80, overlapped	2.85, dd (11.0, 5.6)	2.78, overlapped
15*β*	3.76, dd (15.9, 15.2)	3.75, dd (15.8, 15.1)		2.80, overlapped	2.84, d (11.0)	2.74, overlapped
17	5.12, s	5.12, s	5.23, s	5.73, s	5.77, s	4.97, s
18	1.05, s	1.24, s	1.15, s	1.16, s	1.16, s	1.07, s
19	1.07, s	1.06, s	1.07, s	1.08, s	1.10, s	1.14, s
21				4.98, m	4.97, m	2.33, s
22	7.38, br s	7.35, br s	7.40, br s	6.21, s	6.18, s	
23	6.25, br s	6.24, br s	6.28, br s			
28	0.80, s	0.80, s	0.81, s	0.83, s	0.81, s	0.81, s
29	0.79, s	0.79, s	0.81, s	0.78, s	0.76, s	0.78, s
30	3.31, d (2.2)	3.31, d (2.2)	3.91, d (7.5)	5.34, d (6.8)	5.37, d (6.8)	5.30, d (6.6)
OMe-7	3.72, s	3.73, s	3.70, s	3.69, s	3.69, s	3.66, s
2′	2.74, m	2.55, m			2.61, m	
3''	1.26, d (7.0)	1.76, m 1.51, m	7.05, q (7.1)	6.87, q (7.4)	1.17, d (6.9)	6.91, q (7.0)
4′	1.28, d (7.0)	1.25, d (7.0)	1.95, s	1.83, overlapped	1.18, d (6.9)	1.86, s
5′		0.97, t (7.0)	1.93, d (7.1)	1.83, overlapped		1.88, d (7.0)

[a] Recorded in $CDCl_3$ at 600 MHz for ^{1}H NMR.
[b] Recorded in $CDCl_3$ at 800 MHz for ^{1}H NMR.

thus established and was named 21-deoxo-23-oxofebrifugin A.

Compound **11**, a white amorphous powder, possessed a molecular formula of $C_{31}H_{40}O_9$ as deduced from the negative HRESIMS peak at *m/z* 555.2601 $[M - H]^-$ (calcd. for $C_{31}H_{39}O_9$, 555.2600), showing 12 mass units less than that of **10**. Analysis of the NMR data (Tables 2 and 3) revealed the structure of **11** to be closely related to that of **10**, and the only difference was the substitution at C-3, where an isobutyryloxy group (δ_H 2.61, m; 1.17, d, J = 6.9 Hz; 1.18, d, J = 6.9 Hz; δ_C 176.5, 33.9, 19.2, and 18.5) in **11** was found in place of the tigloyloxy group (6.87, q, J = 7.4 Hz; δ_H 1.83, overlapped; 1.83, overlapped; δ_C 167.0, 139.3, 127.7, 14.8, and 11.9) in **10**. This was further confirmed by the key HMBC correlations from H-3/Me-3′/Me-4′ to C-1′ (Supporting Information Fig. S109). The structure of **11** was thus established and was named 3-*O*-detigloyl-3-*O*-isobutyryl-21-deoxo-23-oxofebrifugin A.

Compound **12**, a white amorphous powder, had the molecular formula of $C_{30}H_{40}O_8$, as determined by the positive HRESIMS ion peak at *m/z* 551.2618 $[M + Na]^+$ (calcd. for $C_{30}H_{40}O_8Na$, 551.2615). Comparison of the 1D NMR data of **12** (Tables 2 and 3) with those of **10** indicated that they shared similar structural skeleton with the major change in ring E. The characteristic *α,β*-unsaturated-γ-lactone ring in **10** was replaced by an acetyl group (δ_H 2.33, s; δ_C 206.8, 28.5) in **12**, which was further confirmed by detailed 2D NMR data (Supporting Information Fig. S119). The acetyl group was attached to C-17 by the HMBC correlations from H-17 (δ_H 4.97) to C-20 (δ_C 206.8)/C-21 (δ_C 28.5), upfield chemical shift of H-17 (δ_H from 5.73 to 4.97), and downfield chemical shift of C-17 (δ_C from 78.0 to 84.3). The structure of **12** was therefore established and was named cipaferen R. To the best of our knowledge, cipaferen R is the first degraded tetranortriterpenoid derivative with an acetyl group at C-17.

The absolute configurations of **1**−**12** including the steroechemistry of C-23 (as in **1**, **2**, **7**, **8**, and **9**) or C-21 (as in **3**, **4**, **5**, and **6**) were determined by comparison of the calculated electronic circular dichroism (ECD) data with their experimental ones, in combination with biosynthetic considerations. The ECD spectra were calculated based on the time-dependent density functional theory (DFT) (Pescitelli and Bruhn, 2016). The DFT reoptimization of the initial Merck molecular force field (MMFF) minima was performed at the B3LYP/6-31 + G (d,p) level with a polarizable continuum model (PCM) solvent model in MeOH. Based on the aforementioned spectroscopic interpretations, the experimental ECD curves of **1** and **2** showed nice agreement with the calculated ECD curve for (2*S*, 3*R*, 5*S*, 9*S*, 10*R*, 13*R*, 14*S*, 17*R*, 23*R*)-**1** (Fig. 3), confirming that **1** and **2** shared the same absolute configuration of (2*S*, 3*R*, 5*S*, 9*S*, 10*R*, 13*R*, 14*S*, 17*R, 23R*). The CD spectra of compounds **1** and **2** showed the split patterns around 214 nm. The positive Cotton effects at λ_{max} 212 nm ($\Delta\varepsilon$ +2.8 for **1**, +0.4 for **2**, π→π* transition) and the negative Cotton effects at about 195 nm ($\Delta\varepsilon$ −43.2 for **1**, −27.6 for **2**, π→π* transition) arising from the exciton coupling of two different chromophores of *α,β*-unsaturated-γ-lactone ring and the $\Delta^{8(30)}$ double bond indicated a positive chirality for both compounds **1** and **2** (Harada and Nakanishi, 1983). The negative absorption at about 300 nm in the ECD spectrum of **1** and **2** are likely resulted from the n→π* transition interaction of the C-3 keto group (Lightner and Gurst, 2000). Briefly, by comparison of the experimental ECD spectra of **3**−**6** with the corresponding calculated ones (Fig. 3), the absolute configurations of **3**−**6** were accordingly assigned as 2*S*, 3*R*, 5*S*, 9*S*, 10*R*, 13*R*, 14*S*, 17*R, 21S*. The absolute configurations of **7**−**12** were accordingly assigned as shown in Fig. 1.

In this study, all the isolates were evaluated for their nematicidal (against the root knot nematode, *Meloidogyne incognita*) and antifungal (against *Fusarium oxysporum* f. sp. *cubense* and *Ralstonia solanacearum*) activities, but no obvious activities were observed. Besides, some isolated compounds (except **2**, **4**, **5**, and **7**–**12** due to insufficient material available) were evaluated for their cytotoxic (against HL-60, SMMC-7721, A-549, MCF-7, and SW-480 human cancer cell lines) and acetylcholinesterase inhibitory activities. 3-*O*-detigloyl-3-*O*-isobutyrylfebrifugin A (**1**), febrifugin A (**13**), febrifugin (**16**), and khaysin

Table 3
^{13}C NMR spectroscopic data for compounds **1–12.**

NO.	1[a]	2[b]	3[a]	4[b]	5[b]	6[b]	7[b]	8[c]	9[c]	10[c]	11[b]	12[c]
1	217.3	217.5	216.3	216.6	216.3	216.9	214.1	214.2	214.3	216.6	216.4	217.5[e]
2	49.1	49.1	48.4	48.9	48.4	49.0	48.8	48.9	48.7	48.8	48.6	49.0
3	77.4	77.2	76.6	77.1	77.3	77.3	76.7	76.8	76.8	77.1	77.3	77.0
4	38.9	38.9	38.5	38.9	38.5	38.8	39.4	39.6	39.8	38.6	38.7	38.9
5	40.6	40.5	41.8	41.8	41.9	41.4	42.5	42.6	41.8	41.7	41.8	41.2
6	33.1	33.1	33.2	33.2	33.4	33.0	33.1	33.2	33.1	32.8	32.8	33.3
7	173.9[e]	173.3	176.4	174.6	176.5	174.1	174.2	174.4	173.6	174.5	174.5	173.7
8	138.0	138.0	137.9	137.9	138.0	137.8	60.5	60.6	60.5	137.4	137.2	138.0[e]
9	56.4	56.5	56.2	56.5	56.2	56.6	55.7	55.9	56.0	56.3	56.2	56.7
10	50.6	50.6	49.5	50.2	49.8	50.1	48.3	48.4	49.2	49.9	50.0	50.5
11	21.1	21.2	20.9	20.7	20.9	20.7	19.3	19.5	21.1	20.4	20.3	20.9
12	34.7	34.8	34.4	34.3	34.5	34.4	32.5	32.7	31.9	34.1	34.1	34.3
13	36.8	36.8	37.4	37.5	37.5	37.5	36.6	36.8	39.2	37.2	37.2	36.8
14	45.5	45.6	45.6	46.2	45.7	45.7	45.9	46.2	161.0	45.3	45.4	45.7
15	29.5	29.5	29.6	29.6	29.9	29.4	34.4	34.5	118.6	29.4	29.6	29.5
16	168.6	168.5	167.9	168.1	168.0	167.2	171.1	171.7[e]	163.5	166.8[e]	167.5	170.5[e]
17	77.3	77.4	76.3	78.3	76.7	78.1	77.3	76.8	76.7	78.0	78.3	84.3
18	22.9	23.0	21.4	22.5	21.7	22.7	26.3	26.6	21.5	15.7	15.6	21.8
19	15.7	15.7	16.1	15.7	16.3	15.9	15.7	15.9	15.9	21.8	21.9	15.6
20	135.5[e]	136.1	163.1	162.0	163.2	161.6	138.1[e]	133.7[e]	134.9[e]	163.8	163.8	206.8[e]
21	168.4[e]	168.3	97.5	104.0	97.7	104.0	169.5[e]	169.2[e]	170.2	72.1	72.1	28.5
22	149.5[d]	147.9	122.2	125.4	122.4	122.0	150.6[d]	150.3[d]	149.7[d]	118.6	118.6	
23	92.0[d]	102.5	169.2	169.5	169.3	169.5	97.0[d]	97.2[d]	96.1[d]	172.2[e]	172.1[e]	
28	21.0	21.1	20.2	20.8	20.2	20.6	21.1	21.2	20.9	20.4	20.6	20.7
29	22.5	22.5	22.7	22.4	22.9	22.9	22.4	22.6	22.9	22.4	22.2	22.6
30	123.3	123.3	123.9	124.0	124.0	124.0	63.4	63.7	62.1	124.2	123.9	123.9
OMe-7	52.3	52.2	53.1	52.4	53.1	52.4	52.4	52.6	52.3	52.4	52.4	52.2
OMe-21				57.2		58.3						
OMe-23		57.6										
1′	176.8	176.8	176.6	176.6	174.2	167.1	176.1	175.7	166.7	167.0[e]	176.5	167.4
2′	34.0	34.0	33.8	33.9	27.1	127.8	34.2	41.7	128.0	127.7	33.9	128.0[e]
3′	18.7	18.7	18.5	18.6	9.0	139.3	19.0	26.8	140.1	139.3	18.5	139.1
4′	19.4	19.4	19.1	19.4		12.0	19.4	17.5	12.5	11.9	19.2	11.9
5′						14.9		12.1	15.0	14.8		14.8

[a] Recorded in $CDCl_3$ at 500 MHz for ^{1}H NMR and 125 MHz for ^{13}C NMR.
[b] Recorded in $CDCl_3$ at 600 MHz for ^{1}H NMR and 150 MHz for ^{13}C NMR.
[c] Recorded in $CDCl_3$ at 800 MHz for ^{1}H NMR and 200 MHz for ^{13}C NMR.
[d] The partial signal observed from HSQC.
[e] The partial signal observed from HMBC.

T (**17**) exhibited moderate cytotoxic activities against the above tested cells with IC_{50} values ranging from 18.56 ± 0.27 to 38.00 ± 0.85 μM (Table 4). 3-*O*-detigloyl-3-*O*-isobutyrylfebrifugin A (**1**), granatumin E (**14**), khaysin T (**17**), and 2′*S*-cipadesin A (**18**) exhibited moderate inhibitory effects against AChE with inhibitory rates of 25.69 ± 1.84%, 23.98 ± 1.55%, 25.13 ± 3.55%, and 38.76 ± 4.33%, respectively, at the concentration of 50 μM (Table 5).

3. Conclusion

A phytochemical study on the petroleum ether fraction of the twigs and leaves of *C. baccifera* led to the isolation of nineteen mexicanolide-type limonoids including twelve previously undescribed limonoids (**1–12**) and seven known analogues (**13–19**). 21-deoxo-23-oxofebrifugin A (**10**) and 3-*O*-detigloyl-3-*O*-isobutyryl-21-deoxo-23-oxofebrifugin A (**11**) are two rare naturally occurring mexicanolide-type limonoids bearing an *α,β*-unsaturated-γ-lactone motif at C-17. Moreover, cipaferen R (**12**) is the first biodegraded tetranortriterpenoid derivative featuring an unique acetyl group at C-17. Among these isolates, no compounds exhibited nematicidal activities against the root knot nematode, *M.incognita* and antifungal activities against *F.oxysporum* f. sp. *cubense* and *R.solanacearum*. However, some compounds exhibited moderate cytotoxic activities against several human cancer cell lines. Structure−activity relationship analysis with compounds **1**, **3**, **6**, and **13–19** indicated that the $\Delta^{8(30)}$ olefinic bond and the substituents at C-3 and C-17 had effect on the cytotoxicity. We also demonstrated that several mexicanolide-type limonoids (**1**, **14**, **17**, and **18**) possessed moderate acetylcholinesterase inhibitory activities. This study not only enriches the chemical diversity of mexicanolide-type limonoids in the Meliaceae family but also forms a basis for the discovery of bioactive natural products from Meliaceae herbs.

4. Experimental

4.1. General experimental procedures

Optical rotations were obtained with a Rudolph Autopol VI polarimeter. UV spectra were measured with a Shimadzu UV-2401A instrument. IR spectra (KBr) were determined on a Bruker Tensor-27 infrared spectrometer. ECD spectra were measured with a Chirascan circular dichroism spectrometer (Applied Photophysics). The NMR spectra were obtained on a Bruker Avance spectrometer operating at 500, 600, and 800 MHz for ^{1}H NMR and 125, 150, and 200 MHz for ^{13}C NMR, using tetramethylsilane as an internal standard. HRESIMS were carried out on a Shimadzu UPLC-IT-TOF mass spectrometer. Semi-preparative HPLC was performed on a Waters 600 pump system with a 2996 photodiode array detector by using a YMC-Pack ODS-A column (300 × 10 mm, S-5 μm). TLC was performed on plates precoated with silica gel GF254 (10–40 μm), while column chromatography (CC) was run over silica gel (200–300 mesh, Qingdao Marine Chemical Factory, Qingdao, China), Sephadex LH-20 gel (40–70 μm, Amersham Pharmacia Biotech AB, Uppsala, Sweden), C18-reversed phase silica gel (250 mesh, Merck), or MCI gel (CHP20/P120, 75–150 μm, high-porous polymer, Mitsubishi Chemical Corporation, Tokyo, Japan). Spots were detected firstly on

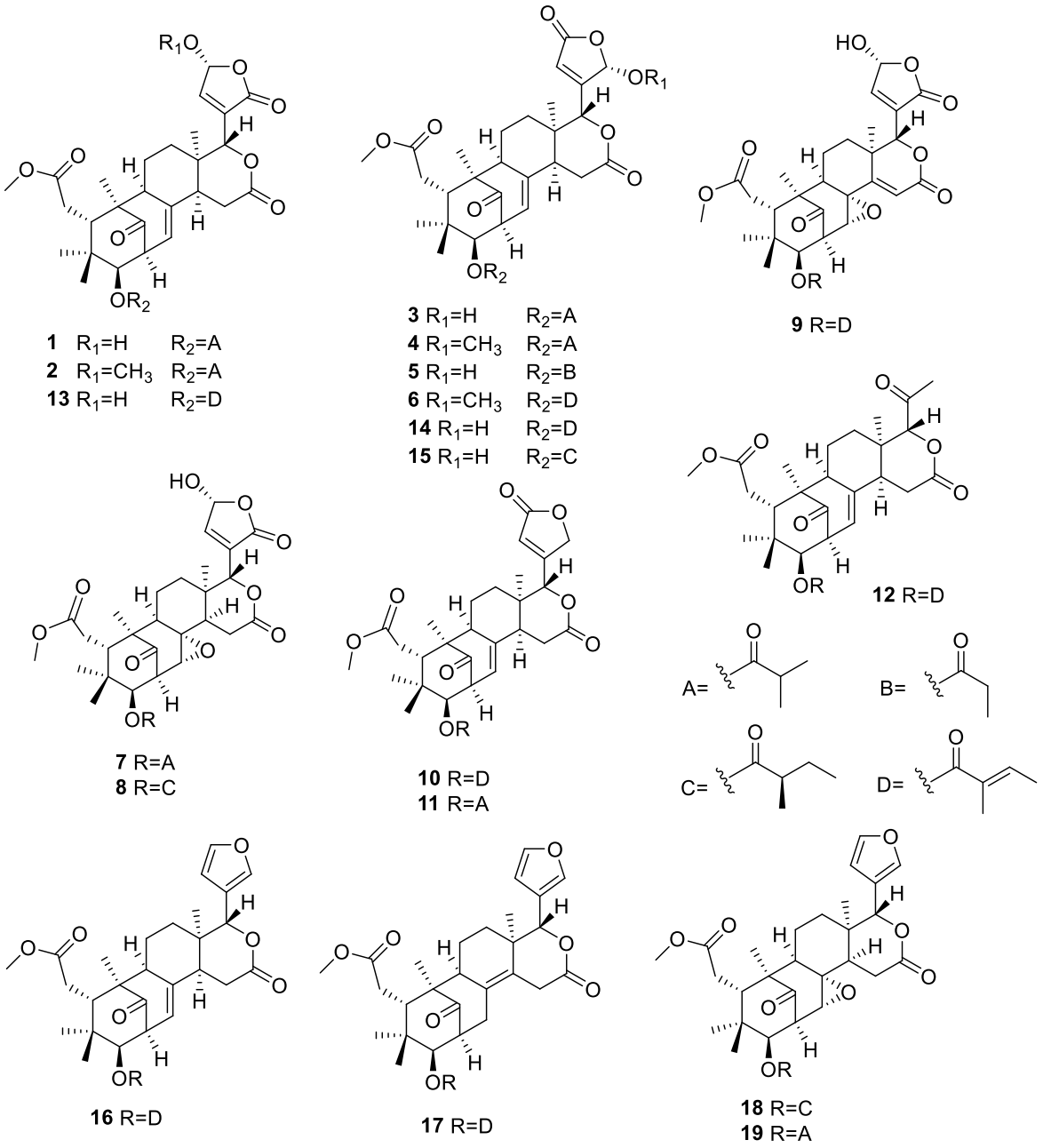

Fig. 1. Structures of compounds **1** – **19**.

TLC (Qingdao Marine Chemical Factory) under 254 nm UV light and then by spraying with 10% H_2SO_4 in ethanol for plate heating. All solvents used were of analytical grade (Shanghai Chemical Reagents Co. Ltd) and all solvents used for HPLC were of chromatographic grade (J & K Scientific Ltd.).

4.2. Plant material

The twigs and leaves of *Cipadessa baccifera* (Roth) Miq. were collected from Xishuangbanna Tropical Botanical Garden, Chinese Academy of Science (101°25′ E,21°41′ N), Mengla Country, Yunnan Province, People's Republic of China at altitude of 570 m in August 2015, and they were identified by one of the authors (Chun-Fen Xiao). A voucher specimen (No. HITBC-058126) is deposited in the herbarium at Xishuangbanna Tropical Botanical Garden, Chinese Academy of Science.

4.3. Extraction and isolation

The air-dried powder of the twigs and leaves of *C. baccifera* (6.8 kg) was extracted with 95% EtOH (40 L) at room temperature three times to afford a crude extract (560 g). The extract was then dissolved in water (2 L) and successively partitioned with petroleum ether (2 L × 3) and EtOAc (2 L × 3). The petroleum ether extract (315 g) was subjected to CC over a D101-macroporous absorption resin eluted with EtOH/H_2O (50%, 80%, and 95%, v/v) to afford three fractions (A, B, and C). Fraction B (80%, 127 g) was subjected to an MCI gel column, eluted with mixtures of MeOH/H_2O (50%–100%, v/v), to give six subfractions (B1 – B6). Fraction B2 (8 g) eluted by 60% MeOH was then separated by silica gel CC ($CHCl_3$/MeOH, 20:1 to 1:2, v/v) to produce five fractions (B2a – B2e). Fraction B2b was further separated by CC over a Sephadex LH-20 (2 cm × 100 cm) column (MeOH as eluent) to give three major subfractions, purification of which by semi-preparative HPLC

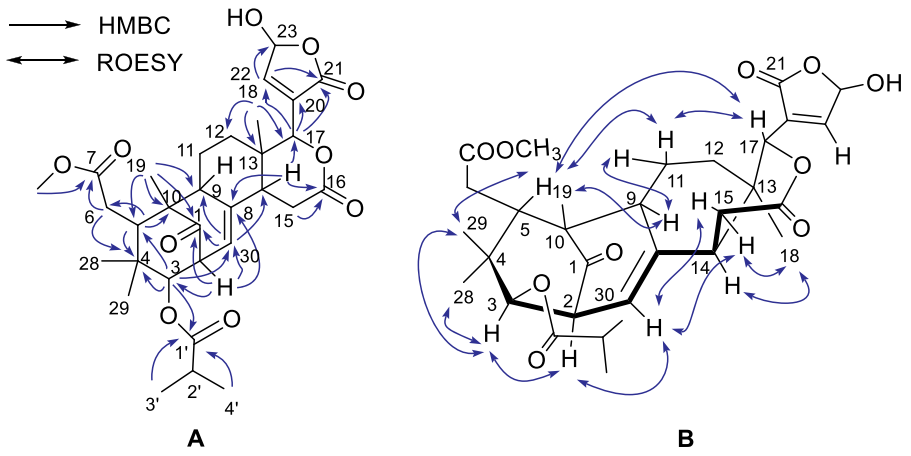

Fig. 2. Key HMBC (A) and ROESY (B) correlations for compound **1**.

(10 mm × 300 mm, MeCN/H_2O, 52:48, v/v, 3 mL/min) yielded compounds **16** (36.0 mg), **18** (24.0 mg), and **19** (10.2 mg), respectively. Using similar procedures, compounds **17** (15.0 mg) and **13** (11.6 mg) were obtained from fraction B2c. Fraction B3 (70%, 28 g) was separated by silica gel CC (petroleum ether/acetone, 50:1 to 1:2, v/v) to give eight fractions (B3a − B3h). Fraction B3e was separated by RP-18 silica gel CC, eluted with MeOH/H_2O (50%–70%, v/v), to yield four subfractions (B3e1 − B3e4). Fraction B3e1 was further separated by silica gel CC ($CHCl_3$/MeOH, 50:1 to 1:1, v/v) to give compounds **1** (12.5 mg) and **3** (8.0 mg). Fraction B3e2 was further separated by silica gel CC ($CHCl_3$/MeOH, 100:1 to 2:1, v/v) to provide four major fractions, purification of which by semi-preparative HPLC (acetonitrile/water) yielded compounds **2** (4.4 mg), **4** (5.0 mg), **5** (5.2 mg), and **6** (4.5 mg), respectively. Fraction B3f (5 g) was then subjected to silica gel CC ($CHCl_3$/MeOH, 50:1 to 1:1, v/v) to give three major fractions (B3f1 − B3f3), purification of which by semi-preparative HPLC using acetonitrile/water as the mobile phase afforded compounds **7** (4.5 mg), **8** (3.0 mg), and **9** (3.6 mg), respectively. Fraction B4 (80%, 54 g) was chromatographed on a silica gel column (6 cm × 70 cm, 200–300 mesh) eluted with gradient mixtures of petroleum ether/acetone (100:0, 50: 1, 20:1, 10:1, 5: 1, 2:1, 1: 1, v/v, each 4 L) to yield seven fractions (B4a–B4g, 5.5, 3.8, 19.2, 12.6, 5.0, 7.6, and 3.2 g, respectively), separation of which by repeated silica gel CC and semi-preparative HPLC (acetonitrile/water, 60:40, v/v, 3 mL/min) yielded compounds **10** (3.8 mg), **11** (5.7 mg), **12** (4.0 mg), **14** (9.0 mg), and **15** (18.0 mg), respectively.

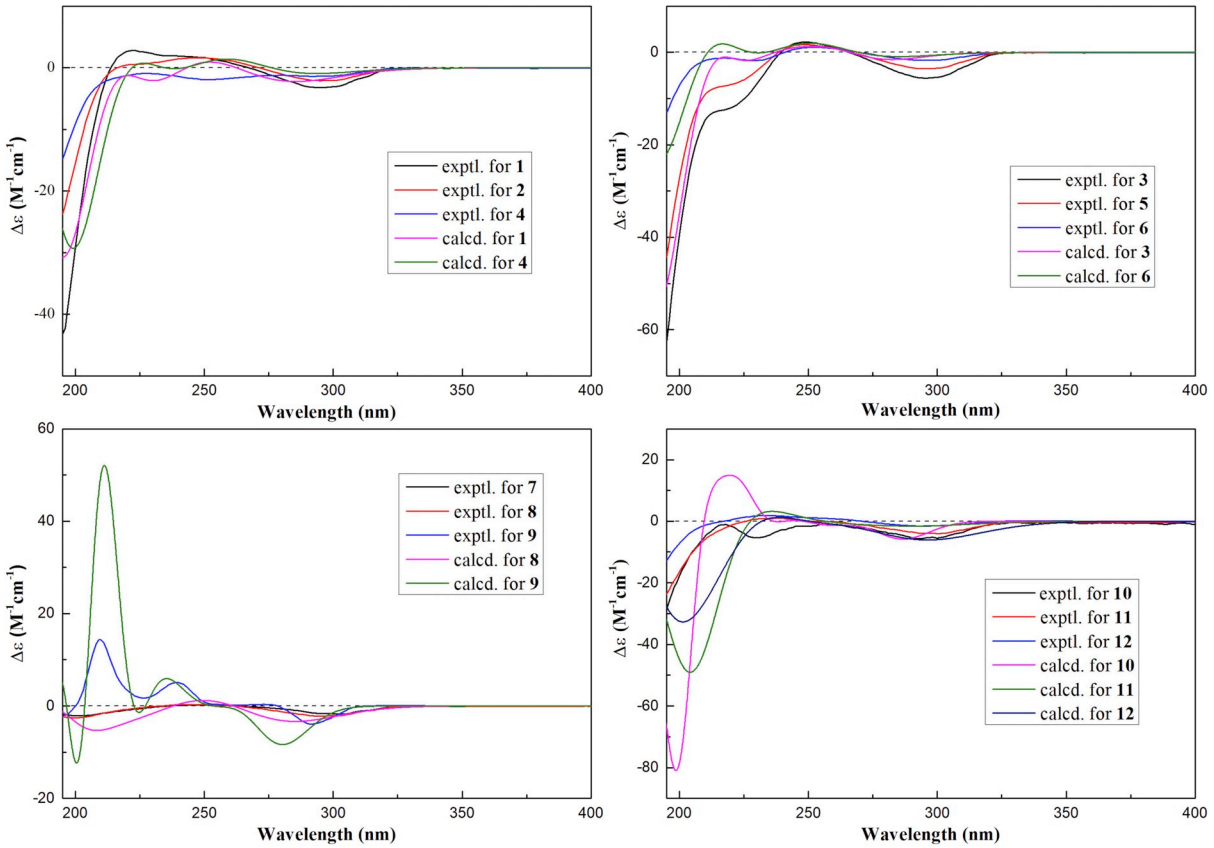

Fig. 3. Experimental and calculated ECD spectra of **1** − **12**.

Table 4
Cytotoxic activity of compounds **1, 3, 6, 13–19** (IC_{50} ± SD, μM).

Compound	HL-60	SMMC-7721	A-549	MCF-7	SW480
1	22.64 ± 1.17	> 40	> 40	> 40	30.34 ± 0.77
3, 6	> 40	> 40	> 40	> 40	> 40
13	20.55 ± 0.24	> 40	> 40	> 40	27.17 ± 0.46
14–15	> 40	> 40	> 40	> 40	> 40
16	18.56 ± 0.27	31.87 ± 0.69	21.25 ± 0.17	24.43 ± 1.48	38.00 ± 0.852
17	30.31 ± 1.41	> 40	> 40	> 40	29.40 ± 1.48
18–19	> 40	> 40	> 40	> 40	> 40
Cisplatin[a]	4.05 ± 0.11	14.91 ± 0.36	19.40 ± 0.71	22.96 ± 0.58	23.15 ± 0.22

[a] Positive control.

Table 5
AChE inhibitory activities of compounds **1–19**[a].

Compound	AChE Inhibition (%) [50 μM]	Compound	AChE Inhibition (%) [50 μM]
1	25.69 ± 1.84	**14**	23.98 ± 1.55
2	N.T.	**15**	16.75 ± 1.70
3	15.47 ± 1.28	**16**	17.77 ± 3.21
4–5	N.T.	**17**	25.13 ± 3.55
6	13.48 ± 1.85	**18**	38.76 ± 4.33
7–12	N.T.	**19**	17.55 ± 1.79
13	14.08 ± 2.24	Tacrine [b]	68.71 ± 0.79

[a] Data are represented as mean ± SEM; N.T.: Not tested.
[b] Calculated percentages of AChE inhibition using tacrine (0.333 μM) as positive control.

*4.3.1. 3-O-detigloyl-3-O-isobutyrylfebrifugin A (**1**)*

White, amorphous powder; $[\alpha]_D^{24.5}$ −87.5 (*c* 0.17, MeOH); UV (MeOH) λ_{max} (log ε): 197 (4.6) nm; IR (KBr) ν_{max}: 3433, 2928, 1770, 1727, 1634, 1458, 1384, 1219, 1149, 1017, 932, 580 cm^{-1}; HRESIMS *m/z* 571.2548 $[M - H]^-$ (calcd. for $C_{31}H_{39}O_{10}$, 571.2549); ^1H NMR ($CDCl_3$), see Table 1 and ^{13}C NMR ($CDCl_3$), see Table 3.

*4. 3.2. 3-O-detigloyl-3-O-isobutyryl-23-O-methylfebrifugin A (**2**)*

White, amorphous powder; $[\alpha]_D^{19.7}$ −83.0 (*c* 0.12, MeOH); UV (MeOH) λ_{max} (log ε): 196 (4.7) nm; IR (KBr) ν_{max}: 3442, 2851, 1774, 1728, 1632, 1458, 1384, 1217, 1028, 991, 585 cm^{-1}; HRESIMS *m/z* 609.2674 $[M + Na]^+$ (calcd. for $C_{32}H_{42}O_{10}Na$, 609.2670); ^1H NMR ($CDCl_3$), see Table 1 and ^{13}C NMR ($CDCl_3$), see Table 3.

*4.3.3. 3-O-detigloyl-3-O-isobutyrylgranatumin E (**3**)*

white, amorphous powder; $[\alpha]_D^{19.3}$ −121.7 (*c* 0.24, MeOH); UV (MeOH) λ_{max} (log ε): 197 (4.1) nm; IR (KBr) ν_{max}: 3436, 2972, 1764, 1727, 1635, 1469, 1384, 1218, 1052, 992, 558 cm^{-1}; HRESIMS *m/z* 571.2546 $[M - H]^-$ (calcd. for $C_{31}H_{39}O_{10}$, 571.2549); ^1H NMR ($CDCl_3$), see Table 1 and ^{13}C NMR ($CDCl_3$), see Table 3.

*4.3.4. 3-O-detigloyl-3-O-isobutyryl-21-O-methylgranatumin E (**4**)*

White, amorphous powder; $[\alpha]_D^{19.7}$ −118.7 (*c* 0.11, MeOH); UV (MeOH) λ_{max} (log ε): 195 (4.6) nm; IR (KBr) ν_{max}: 3432, 2923, 1771, 1728, 1632, 1468, 1384, 1216, 1048, 993, 585 cm^{-1}; HRESIMS *m/z* 609.2668 $[M + Na]^+$ (calcd. for $C_{32}H_{42}O_{10}Na$, 609.2670); ^1H NMR ($CDCl_3$), see Table 1 and ^{13}C NMR ($CDCl_3$), see Table 3.

*4.3.5. 3-O-detigloyl-3-O-propanoylgranatumin E(**5**)*

White, amorphous powder; $[\alpha]_D^{19.8}$ −113.6 (*c* 0.19, MeOH); UV (MeOH) λ_{max} (log ε): 196 (4.6) nm; IR (KBr) ν_{max}: 3435, 2973, 1765, 1727, 1632, 1436, 1344, 1218, 1051, 973, 559 cm^{-1}; HRESIMS *m/z* 581.2359 $[M + Na]^+$ (calcd. for $C_{30}H_{38}O_{10}Na$, 581.2357); ^1H NMR ($CDCl_3$), see Table 1 and ^{13}C NMR ($CDCl_3$), see Table 3.

*4.3.6. 21-O-methylgranatumin E (**6**)*

White, amorphous powder; $[\alpha]_D^{20.1}$ −71.9 (*c* 0.12, MeOH); UV (MeOH) λ_{max} (log ε): 195 (4.6) nm; IR (KBr) ν_{max}: 3439, 2957, 1769, 1728, 1631, 1458, 1384, 1261, 1053, 992, 548 cm^{-1}; HRESIMS *m/z* 597.2707 $[M-H]^-$ (calcd. for $C_{33}H_{41}O_{10}$, 597.2705); ^1H NMR ($CDCl_3$), see Table 1 and ^{13}C NMR ($CDCl_3$), see Table 3.

*4.3.7. 21-oxo-23-hydroxylruageanin A (**7**)*

White, amorphous powder; $[\alpha]_D^{20.5}$ −101.7 (*c* 0.09, MeOH); UV (MeOH) λ_{max} (log ε): 195 (4.5), 277 (3.5) nm; IR (KBr) ν_{max}: 3435, 2924, 1773, 1732, 1631, 1437, 1384, 1260, 1040, 991, 582 cm^{-1}; HRESIMS *m/z* 587.2498 $[M - H]^-$ (calcd. for $C_{31}H_{39}O_{11}$, 587.2498); ^1H NMR ($CDCl_3$), see Table 2 and ^{13}C NMR ($CDCl_3$), see Table 3.

*4.3.8. 3-O-detigloyl-3-O-(2′R-methylbutanoyl)-21-oxo-23-hydroxylruageanin A (**8**)*

White, amorphous powder; $[\alpha]_D^{20.1}$ −113.5 (*c* 0.08, MeOH); UV (MeOH) λ_{max} (log ε): 195 (4.6) nm; IR (KBr) ν_{max}: 3437, 2924, 1772, 1732, 1632, 1460, 1384, 1260, 1025, 989, 584 cm^{-1}; HRESIMS *m/z* 601.2654 $[M - H]^-$ (calcd. for $C_{32}H_{41}O_{11}$, 601.2654); ^1H NMR ($CDCl_3$), see Table 2 and ^{13}C NMR ($CDCl_3$), see Table 3.

*4.3.9. 3-O-deisobutyryl-3-O-tigloyl-14,15-dedihydro-21-oxo-23-hydroxylruageanin A (**9**)*

White, amorphous powder; $[\alpha]_D^{20.6}$ −33.1 (*c* 0.11, MeOH); UV (MeOH) λ_{max} (log ε): 195 (4.4) nm; IR (KBr) ν_{max}: 3440, 2918, 1769, 1730,1646, 1456, 1384, 1262, 1045, 955, 609 cm^{-1}; HRESIMS *m/z* 597.2345 $[M - H]^-$ (calcd. for $C_{32}H_{37}O_{11}$, 597.2341); ^1H NMR ($CDCl_3$), see Table 2 and ^{13}C NMR ($CDCl_3$), see Table 3.

*4.3.10. 21-deoxo-23-oxofebrifugin A (**10**)*

White, amorphous powder; $[\alpha]_D^{20.6}$ −115.5 (*c* 0.06, MeOH); UV (MeOH) λ_{max} (log ε): 196 (4.5) nm; IR (KBr) ν_{max}: 3438, 2920, 1773, 1728, 1634, 1466, 1384, 1261, 1052, 890, 558 cm^{-1}; HRESIMS *m/z* 567.2600 $[M - H]^-$ (calcd. for $C_{32}H_{39}O_9$, 567.2600); ^1H NMR ($CDCl_3$), see Table 2 and ^{13}C NMR ($CDCl_3$), see Table 3.

*4.3.11. 3-O-detigloyl-3-O-isobutyryl-21-deoxo-23-oxofebrifugin A (**11**)*

White, amorphous powder; $[\alpha]_D^{20.6}$ −72.9 (*c* 0.09, MeOH); UV (MeOH) λ_{max} (log ε): 196 (4.4) nm; IR (KBr) ν_{max}: 3436, 2921, 1774, 1730, 1633, 1467, 1384, 1261, 1051, 995, 560 cm^{-1}; HRESIMS *m/z* 555.2601 $[M - H]^-$ (calcd. for $C_{31}H_{39}O_9$, 555.2600); ^1H NMR ($CDCl_3$), see Table 2 and ^{13}C NMR ($CDCl_3$), see Table 3.

*4.3.12. Cipaferen R (**12**)*

White, amorphous powder; $[\alpha]_D^{19.5}$ −39.4 (*c* 0.13, MeOH); UV (MeOH) λ_{max} (log ε): 196 (4.5), 271 (3.0) nm; IR (KBr) ν_{max}: 3443, 2918, 1731, 1636, 1467, 1383, 1261, 1026, 999, 558 cm^{-1}; HRESIMS *m/z* 551.2618 $[M + Na]^+$ (calcd. for $C_{30}H_{40}O_8Na$, 551.2615); ^1H NMR ($CDCl_3$), see Table 2 and ^{13}C NMR ($CDCl_3$), see Table 3.

4.4. In vitro screening for nematicidal activity

The root-knot nematode *M. incognita* was selected for nematicidal bioassay. Second stage juveniles (J2s) of *M. incognita* were collected to

prepare the nematode suspension based on the protocol reported previously (Li et al., 2014), with minor modifications. The obtained compounds (**1**–**19**) were dissolved and diluted in DMSO to obtain sample solvents at 10 mg/mL.

For nematicidal bioassay, 5 μL sample solvent was mixed with 495 μL J2 suspension, containing about 100 J2s, and then added into a well in 12-well microtitre plates. Wells containing DMSO served as negative controls, while fosthiazate served as positive control. Each treatment was replicated thrice. After incubation at 28 °C for 72 h, suspensions were centrifuged at 4193 g for 1 min to remove the liquid portion. The nematodes were resuspended in tap water for 30 min to check their potential for revival. Numbers of live and dead nematodes were counted under a stereomicroscope. The experiment was repeated three times under the same conditions.

4.5. Antifungal assay

The obtained compounds were evaluated for their antifungal activity using a disk diffusion method as described in the literature (Zheng et al., 2018). Fungal species (*F.oxysporum* f. sp. *cubense* and *R. solanacearum*) were obtained from Yunnan University. 10 mL sterile liquid PDA medium, mixed with freshly homogenized fungus at 40 °C, was poured into Petri dishes (9 cm in diameter) and allowed to solidify. Test compounds were dissolved in ethanol with the final concentration of 5 mg/mL. The sterile filter paper disk (6 mm in diameter) was soaked with 10 μL test solution and placed onto the above PDA plate containing fungus. Nystatin was used as positive control for antifungal activity. A disk containing ethanol was used as negative control. The Petri dish was sealed with parafilm and incubated at 26 °C. The diameter of inhibition zone was measured after 72 h. Each test had three replicates.

4.6. Cytotoxicity assay

The obtained compounds were tested for their cytotoxic activity against the HL-60, SMMC-7721, A-549, MCF-7, and SW480 cancer cell lines using the MTS method. Briefly, all cells were cultured in RPMI 1640 medium containing 10% fetal bovine serum and 100 U/mL penicillin/streptomycin in a humidified incubator in a 5% CO_2 atmosphere at 37 °C. Then, 100 μL adherent cells was seeded into each well (1 × 104 cells/well) of 96-well cell culture plates and allowed to adhere for 12 h before test drug addiction. Each tumor cell line was exposed to a test compound at concentrations of 0.064, 0.32, 1.6, 8, and 40 μM in DMSO in triplicate for 48 h, with cisplatin as the positive control. After 48 h incubation, 20 μL MTS [3-(4,5-dimethylthiazol-2-yl)-5-(3-carboxymethoxy-phenyl)-2-(4-sulfophenyl)-2H-tetrazolium] solution was added to each well, which were incubated for another 4 h to give a formazan product. Then, 100 μL 20% SDS was added to each well and incubated 12 h at room temperature for the formazan product to dissolve completely. The OD value of each well was measured at 490 nm using a Biorad 680 instrument. The IC50 value of each compound was calculated by the Reed and Muench method (Reed and Muench, 1938).

4.7. Acetylcholinesterase inhibitory activity

Acetylcholinesterase (AChE) inhibitory activity of the isolated compounds was assayed by the spectrophotometric method developed by Ellman et al. (1961), with slight modifications. *S*-Acetylthiocholine iodide, 5,5′-dithio-bis-(2-nitrobenzoic) acid (DTNB, Ellman's reagent), and acetylcholinesterase derived from human erythrocytes were purchased from Sigma Chemical. These compounds were dissolved in DMSO. The reaction mixture (totally 200 μL) containing phosphate buffer (pH 8.0), the test compound (50 μM), and acetyl cholinesterase (0.02 U/mL) was incubated for 20 min (37 °C). Then, the reaction was initiated for AChE inhibitory activity assay by addition of 20 μL solution containing DTNB (0.625 mM) and 20 μL acetylthiocholine iodide (0.625 mM). Hydrolysis of acetylthiocholine was monitored at 405 nm every 30 s for 1 h. Tacrine was used as the positive control with final concentration of 0.333 μM. All the reactions were performed in triplicate. The percentage inhibition was calculated as follows: % inhibition = (E − S)/E × 100, where E is the absorbance at 405 nm of the solution without the test compound and S is the absorbance at 405 nm of the solution with the test compound.

Declaration of competing interest

The authors declare no conflict of interest.

Acknowledgments

This work was supported financially by Systematic Evaluation of Ethnic Medicinal Plant Resources in Tropical Regions and Development of Health Products for the Public (2017XTBG-F02), Conservation and Application of National Strategic Tropical Plant Resources: Theory and Practice (2017XTBG-F05), and the International Partnership Program of Chinese Academy of Sciences (153631KYSB20160004). Special thanks are given to the UCAS Joint PhD Training Program, PhD. Mo Minghe, a professor at Yunnan University, and the Central Laboratory of XTBG for the technical support of this study.

Appendix A. Supplementary data

Supplementary data to this article can be found online at https://doi.org/10.1016/j.phytochem.2020.112449.

References

Bandi, A.K.R., Lee, D.U., 2012. Secondary metabolites of plants from the genus *Cipadessa*: chemistry and biological activity. Chem. Biodivers. 9, 1403–1421.
Chen, S.K., Chen, B.Y., Li, H., 1997. Chinese Flora (Zhongguo Zhiwu Zhi), vol. 43. Science Press, Beijing, pp. 60.
Ellman, G.L., Courtney, K.D., Andres Jr., V., Featherstone, R.M., 1961. A new and rapid colorimetric determination of acetylcholinesterase activity. Biochem. Pharmacol. 7, 88–95.
Gan, L.S., Wang, X.N., Wu, Y., Yue, J.M., 2007. Tetranortriterpenoids from *Cipadessa baccifera*. J. Nat. Prod. 70, 1344–1347.
Harada, N., Nakanishi, K., 1983. Circular Dichroic Spectroscopy—Exciton Coupling in Organic Stereochemistry. University Science Books (Mill Valley).
Jiangsu New Medical College, 1977. Dictionary of Chinese Materia Medica. Shanghai Science and Technology Press, Shanghai 2, pp. 2183.
Leite, A.C., Fernandes, J.B., da Silva, M., Vieira, P.C., 2005. Limonoids from *Cipadessa fruticosa*. Z. Naturforsch. B Chem. Sci.: Biosci. 60, 351–355.
Li, G.J., Dong, Q.E., Ma, L., Huang, Y., Zhu, M.L., Ji, Y.P., Wang, Q.H., Mo, M.H., Zhang, K.Q., 2014. Management of *Meloidogyne incognita* on tomato with endophytic bacteria and fresh residue of *Wasabia japonica*. J. Appl. Microbiol. 117, 1159–1167.
Li, M.Y., Yang, X.B., Pan, J.Y., Feng, G., Xiao, Q., Sinkkonen, J., Satyanandamurty, T., Wu, J., 2009. Granatumins A − G, limonoids from the seeds of a krishna mangrove, *Xylocarpus granatum*. J. Nat. Prod. 72, 2110–2114.
Liao, S.G., Chen, H.D., Yue, J.M., 2009. Plant orthoesters. Chem. Rev. 109, 1092–1140.
Lightner, D.A., Gurst, J.E., 2000. Organic Conformational Analysis and Stereochemistry from Circular Dichroism Spectroscopy. Wiley, New York.
Malarvannan, S., Giridharan, R., Sekar, S., Prabavathy, V., Nair, S., 2009. Ovicidal activity of crude extracts of few traditional plants against *Helicoverpa armigera* (Hubner) (Noctuidae: Lepidoptera). J. Biopestic. 2, 64–71.
Mootoo, B.S., Ramsewak, R., Khan, A., Tinto, W.F., Reynolds, W.F., McLean, S., Yu, M., 1996. Tetranortriterpenoids from *Ruagea glabra*. J. Nat. Prod. 59, 544–547.
Pennington, T.D., Styles, B.T., 1975. A generic monograph of the Meliaceae. Blumea 22, 419–540.
Pescitelli, G., Bruhn, T., 2016. Good computational practice in the assignment of absolute configurations by TDDFT calculations of ECD spectra. Chirality 28, 466–474.
Ram, A.J., Bhakshu, L.M., Raju, R.V., 2004. *In vitro* antimicrobial activity of certain medicinal plants from eastern ghats, India, used for skin diseases. J. Ethnopharmacol. 90, 353–357.
Rao, M.M., Krishna, E.M., Gupta, P.S., Singh, P.P., 1978. New tetranortriterpenoid isolated from heartwood of *Soymida febrifuga*. Indian J. Chem. B 16, 823–825.
Reed, L., Muench, H., 1938. A simple method for determining 50 per cent endpoints. Am. J. Hyg. 27, 493–497.
Siva, B., Poornima, B., Venkanna, A., Prasad, K.R., Sridhar, B., Nayak, V.L., Ramakrishna, S., Babu, K.S., 2014. Methyl angolensate and mexicanolide-type limonoids from the seeds of *Cipadessa baccifera*. Phytochemistry 98, 174–182.

Siva, B., Venkanna, A., Poornima, B., Divya, R.S., Boustie, J., Bastien, S., Jain, N., Usha, R.P., Suresh, B.K., 2017. New seco-limonoids from *Cipadessa baccifera*: isolation, structure determination, synthesis and their antiproliferative activities. Fitoterapia 117, 34.

Sun, D.M., An, F.L., Wei, S.S., Zhang, Y.Q., Wang, X.B., Luo, J., Kong, L.Y., 2018. Cipadessains A−K, eleven limonoids from the fruits of *Cipadessa cinerascens*. RSC Adv. 8 (19), 10437–10445.

Tan, Q.G., Luo, X.D., 2011. Meliaceous limonoids: chemistry and biological activities. Chem. Rev. 111, 7437–7522.

Wang, H.Y., Wang, J.S., Shan, S.M., Wang, X.B., Luo, J., Yang, M.H., Kong, L.Y., 2013. Chemical constituents from *Trichilia connaroides* and their nitric oxide production and α-glucosidase inhibitory activities. Planta Med. 79, 1767–1774.

Yu, J.H., Wang, G.C., Han, Y.S., Wu, Y., Wainberg, M.A., Yue, J.M., 2015. Limonoids with anti-HIV activity from *Cipadessa cinerascens*. J. Nat. Prod. 78, 1243–1252.

Yu, J.H., Zhou, B., Dalal, S., Liu, Q.F., Cassera, M.B., Yue, J.M., 2018. Cipaferoids A−C, three limonoids represent two different scaffolds from *Cipadessa baccifera*. Chin. J. Chem. 36, 124–128.

Zheng, G.W., Luo, S.H., Li, S.F., Hua, J., Li, W.Q., Li, S.H., 2018. Specialized metabolites from *Ageratina adenophora* and their inhibitory activities against pathogenic fungi. Phytochemistry 148, 57–62.